Integrating MPC with Learning-Based and Adaptive Methods to Enhance Safety, Performance and Reliability in Automated Insulin Delivery [1]

Iman Hajizadeh [†] **Mohammad Reza Askari** [†] **Ranjeet Kumar** [‡]
Victor M. Zavala [‡] **Ali Cinar** [†,2]

[†] *Department of Chemical and Biological Engineering,*
Illinois Institute of Technology, Chicago, IL, USA
[‡] *Department of Chemical and Biological Engineering,*
University of Wisconsin-Madison, Madison, WI, USA

Abstract: In this work, an adaptive-learning model predictive control (AL-MPC) framework that integrates disturbance forecasting, uncertainty quantification, learning, and recursive subspace identification is developed. The proposed technique can be used for continuous systems affected by repetitive disturbances with unknown periods. The AL-MPC integrates online learning from historical data to anticipate impending disturbances and proactively counteract their effects to an adaptive MPC. This is done by using machine learning to quantify the significant disturbances from historical data and forecast their future evolution time series. Behavior patterns of the system can be identified from historical data, and the set-point, objective function weights, and constraints of the controller can be modified in advance for the anticipated time periods of the disturbance effects. AL-MPC is used to regulate glucose concentration (GC) in people with diabetes by automated insulin delivery. Simulation results indicate that the AL-MPC can regulate the BGC 75.4% of the simulation time in the target range (70-180) mg/dL without causing any hypoglycemia and hyperglycemia events.

Keywords: Adaptive model predictive control, Diabetes, Automated insulin delivery, Machine learning, Recursive system identification

1. INTRODUCTION

Control of systems with time-varying parameters and non-linear dynamics is challenging. The presence of stochastic disturbances, random measurement noises and unknown time-varying delays can make the control of such processes more complex. Time-invariant models cannot describe the dynamic behavior of these processes accurately. Furthermore, offline-tuned controllers cannot perform satisfactorily when the process is subjected to major disturbances. Model predictive control (MPC) is widely employed in many fields due to its inherent ability to effectively handle multivariable complex systems with different constraints (Garcia et al. (1989); Rawlings and Mayne (2009); Zavala and Biegler (2009); Mesbah et al. (2017); Ganesh et al. (2016); Moharir et al. (2018); Perea-Lopez et al. (2003); Mayne (2014); Hajizadeh et al. (2019b); Garcia-Tirado et al. (2019)). MPC algorithms use the dynamic model of the system in the optimization problem to predict the future evolution of the outputs over a finite-time horizon to determine the optimal manipulated variables with respect to a specified performance index. Besides, MPC can explicitly consider the system constraints in the optimization problem, and its formulations are not restricted by the type of model, objective function, or constraints. However, the accuracy of the model, the formulation of the objective function, system constraints, and the forecast of unknown stochastic disturbances for use in output predictions affect the MPC performance (Forbes et al. (2015); Kumar et al. (2018); Kumar et al. (2019a,b)).

In a standard MPC implementation, a deterministic representation of uncertain disturbances (i.e., a forecast) is used in the computation of control actions. The forecast acts as a summarizing statistic of the entire disturbance uncertainty space. It is typically the most likely realization of the disturbance (usually the mean) or a constant value. Stochastic MPC (sMPC) formulations have been developed because of the inability to handle disturbances that cannot be adequately represented by the most likely forecasts (Kumar et al. (2018); Kumar et al. (2019a,b)). In sMPC, one often uses historical data to create uncertainty characterizations of the model disturbances and uses such characterizations to generate the most probable scenarios for the evolution of the outputs over the prediction horizon. Consequently, the sMPC provides a more systematic

[2] Correspondence concerning this article should be addressed to A. Cinar at cinar@iit.edu

framework to account for diverse disturbances, satisfy constraints, and maximize control performance.

Historical data can be leveraged to integrate machine learning techniques with MPC to improve the controller performance. In order to improve the output predictions over the prediction horizon of the MPC, the most probable scenarios (as time series forms) need to be utilized in the controller for process disturbances. Our goal is to quantify these significant disturbances and forecast their future evolution by using historical data and machine learning techniques. Furthermore, the historical data can be also utilized to identify the behavior patterns of the underlying system. The controller set-point, weights in the MPC objective function, and system constraints can be modified in advance for the anticipated time periods of the disturbance effects.

In this work, a novel approach based on k-means clustering method is used for disturbance forecasting and uncertainty quantification from historical operational data. k-means clustering is an unsupervised method of vector quantization. It partitions n observations into k clusters where each observation belongs to the cluster with the shortest distance between the observation and the center of that cluster, serving as a representative of the cluster (Wagstaff et al. (2001); Kanungo et al. (2002); Hartigan and Wong (1979)).

Historical data can be also used to identify the various behavior patterns of the system. Incorporating online learning of the probable times of unknown disturbances from the historical data by using k-means algorithm can improve the controlled system performance by proactively mitigating the effects of impending disturbances. In this work, the controller set-point is modified in advance for the anticipated periods of the disturbance effects. It is set at 110 mg/dL except during exercise periods when it becomes 160 mg/dL. The weights in the MPC objective function and the system constraints are also adjusted according to the predicted controller set-point values (Hajizadeh et al. (2019a)). To detect rapid deviations from the desired trajectories caused by significant disturbances in real-time, a feature extraction method (qualitative trend analysis) based on outputs measurements is also designed (Cheung and Stephanopoulos (1990)). The key parameters of the MPC optimization problem are adjusted by using the results of feature extraction. The feature extraction scheme provides information about the rate and shape of variations in outputs to improve the effectiveness of the controller when the presence of major disturbances is detected.

To guarantee that the underlying model can provide accurate output predictions for use in MPC algorithms, we extended the optimized version of the recursive predictor-based subspace identification method (Houtzager et al. (2012)) to obtain a stable time-varying state space model of the system. This is done by the incorporation of constraints on the fidelity and accuracy of the identified models, the correctness of the sign of the input-to-output gains, and the integration of heuristics to ensure the stability of the recursively identified models (Hajizadeh et al. (2018b,a)).
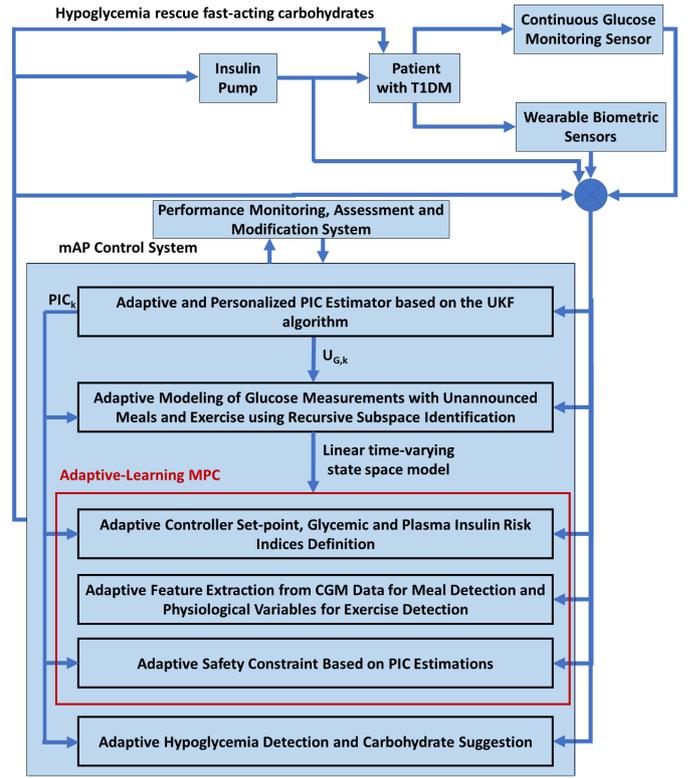

Fig. 1. Flow chart of the proposed mAP Hajizadeh et al. (2019d)

The performance of the developed approach is illustrated by regulating the glucose concentrations (GC) in people with type 1 diabetes (T1D) by means of controlled insulin delivery with artificial pancreas (AP) systems (Hajizadeh et al. (2019b,c)). A general flowchart of our multivariable artificial pancreas (mAP) system is shown in Fig. 1. Biomedical systems are complex dynamical systems with significant uncertainties and exogenous disturbances that provide challenging modeling and control problems. The human body, a time-varying system with nonlinear behavior, is affected by several stochastic and unknown disturbances. Using a multivariable simulation platform for T1D (Rashid et al. (2019)), the adaptive stochastic predictive control with recursive subspace identification and learning is applied to the problem of regulating GC. The case studies illustrate a significant improvement in the AP system performance, and the potential in developing a fully automated AP that can function without making any manual ientriessuch as meal and exercise information and accommodate major disturbances to the GC such as meals and physical activities.

2. PRELIMINARIES

In this section, a brief overview of the recursive subspace system identification technique for the identification of linear, time-varying state-space models, the prediction of the process disturbances using k-means method, and the formulation of the AL-MPC is provided.

2.1 Recursive Subspace-Based System Identification

A stable and accurate dynamic model is essential for the design of MPC algorithms in AP systems. Treating the glu-

cose insulin dynamics as a time-varying linear system, the modified predictor-based subspace identification approach is implemented to track its behavior and is coupled with a constrained optimization solver to guarantee the stability and fidelity of the model (Hajizadeh et al. (2018b,a)).

The proposed recursive system identification technique provides a time-varying stable state space model. It updates parameters of state-space matrices on-line. After integrating the state space model with a physiological insulin compartment model (Hajizadeh et al. (2018a)), the final identified glycemic model for use in an adaptive MPC becomes:

$$\hat{x}_{k+1} = A_k\hat{x}_k + B_ku_k + d_k$$
$$\hat{y}_k = C_k\hat{x}_k \tag{1}$$

where A_k, B_k, and C_k are the system matrices, and d_k represents unmodeled/unmeasured disturbances. For the proposed model, continuous glucose measurement (CGM) is considered as output, and infused insulin information, estimates of the meal effect, and physiological variables represent inputs to indicate physical activity ($u_k = [Ins_k, Meal_k, MET_k]$). MET is the metabolic equivalent of task that represents energy expenditure, as an indicator of the intensity of physical activity. One of the states of the model described by Eq.(1) is the amount of insulin in the bloodstream, called the plasma insulin concentration (PIC). The PIC safety constraints are then defined in the MPC to assure that a safe amount of insulin is in the body.

2.2 Prediction of Disturbances Using k-means Method

In Eq. 1, the infused insulin information is the manipulated variable while estimates of the meal effect, physiological variables, and d_k which is the unmodeled/unmeasured disturbances are unknown disturbances affecting the underlying system. In this work, it is desired to predict these disturbances using historical data using machine learning techniques. The historical data used in machine learning are: i) CGM measurements, ii) infused insulin pump data, iii) estimates of meal effect, iv) physiological variables to indicate physical activity, v) PIC estimates, vi) first and second derivatives of the controlled variable (CGM measurements) to detect (specify) the occurrence of significant disturbances in the historical data, and vii) d values (Hajizadeh et al. (2019a)).

Assume that N days of the historical data are present as shown in Fig. 2. We would like to compare the current trend of data (current evolving pattern) with the historical measurements to find the closest (most similar) scenarios for the forecast of unknown and unmodeled disturbances that include: $Meal$, MET, and d (as is shown in Fig. 3). The first step toward finding the most probable and worst case scenarios for the future disturbances is to find several hyper partitions to categorize unknown disturbances based on their similarities and distances. To achieve this, we construct the training matrix as

$T_{past} = [CGM_{k,n_d}, \dot{CGM}_{k,n_d}, \ddot{CGM}_{k,n_d}, d_{k,n_d}, Meal_{k,n_d},$
$Ins_{k-1,n_d-1}, \hat{PIC}_{k,n_d}, MET_{k,n_d}] \in R^{NL \times M}$.
where $CGM_{k,n_d} = [CGM_k, ..., CGM_{k-n_d}] \in R^{n_d+1}$ is the vector of past CGM values. Similarly, $\dot{CGM}_{k,n_d}$, $\ddot{CGM}_{k,n_d}$, d_{k,n_d}, $Meal_{k,n_d}$, Ins_{k-1,n_d}, $\hat{PIC}_{k,n_d}$, and
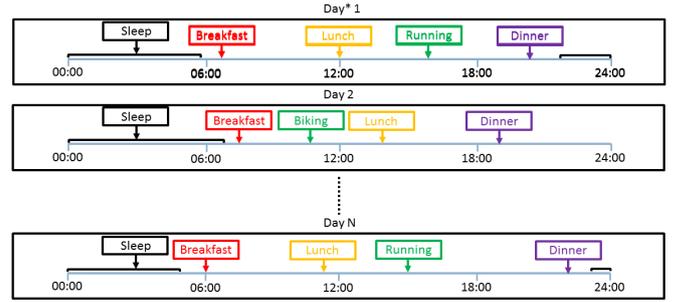
Fig. 2. Historical data processing

MET_{k,n_d} denote the vector of the first and second derivatives of past CGM values, other estimated uncertainties, the effect of meal, the amount of infused insulin, the estimated PIC, and the MET value representing physical activity, respectively. Parameter L is the number of recorded samples per day, $n_d > 1$ is the number of past measurements used in k-means clustering technique, and M denotes the total number of features. Columns of feature variables always come in different orders of magnitudes which may cause biased partitioning results from k-means clustering technique. Hence, before employing k-means, online Z-score data normalization is utilized to scale the training matrix of data to give equal weights to each column of feature variables. For Euclidean distance metrics and a suitable number of clusters ($k \geq 2$), it is desired to minimize the sum of squared error (SSE) function defined as

$$SSE = \sum_{i=1}^{k} \sum_{x \in c_i} (C_i - x)^2. \tag{2}$$

where $C_i \in R^M$ denote the center of each cluster. Obviously, the daily behaviour of the subject significantly affects the pattern of the current data and the number of natural subgroups due to augmenting upcoming samples to the training set. With this in mind, determining the proper number of clusters is crucial step to avoid predicting inaccurate or misleading forecasts of disturbances. In this study we have used Silhouette index to determine the most suitable number of clusters. The average of Silhouette coefficients is calculated for several number of clusters and the k-means model with the maximum average of Silhouette index is chosen for disturbance partitioning. The prediction of probable upcoming disturbances is performed by using the following steps:

I. The cluster with the minimum Euclidean distance between the center of that cluster and the current sample is chosen.
II. Using the selected cluster in step I, the most probable scenario for upcoming disturbances is obtained by averaging the future trends of process disturbances.
III. In order to take into account the possible intense disturbances, two forecasts for process disturbances are selected from cases that their output values (controlled variables) show extreme behaviors over the future window in the selected cluster. These selections make the controller more robust against worse case scenarios.
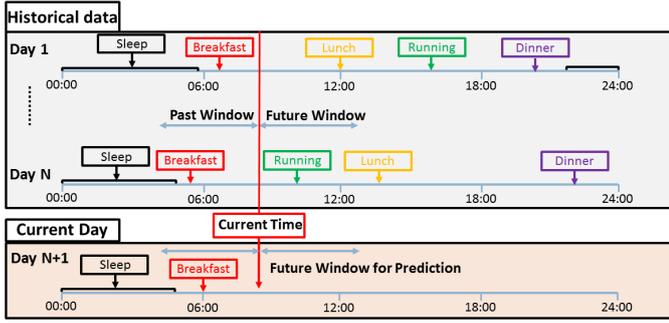
Fig. 3. Pattern recognition using historical data

2.3 Adaptive-Learning MPC Algorithm

The PIC-cognizant AL-MPC computes the optimal insulin infusion rate by utilizing adaptive weights that adjust the penalty weighting matrices in the objective function. It computes the optimal insulin infusion rate over a finite horizon by using the identified time-varying subspace-based models and three different forecasts obtained for the unknown process disturbances by solving a quadratic programming problem at each sampling time k:

$$\left\{z_{i,j}^*, m_{i=0}^{*n_P}\right\} := \underset{m \in \mathcal{M}, z_j \in \mathcal{Z}}{\arg\min} \mathcal{J}_{n_P,k}(Q_{j,k}, R_k, m_{i=0}^{n_P}, z_{j,i=0}^{n_P})$$

$$\text{s.t.} \begin{cases} z_{j,i+1} = A_k z_{j,i} + B_k m_i + d_{j,i} \\ q_{j,i} = C_k z_{j,i} \\ z_{j,0} = \hat{x}_{j,k} \\ m_{j,i}^{min} \le m_i \le m_{j,i}^{max} \\ z_{j,i}^{PIC,min} \le z_{j,i}^{PIC} \le z_{j,i}^{PIC,max} \\ e_{j,i}^{PIC} = z_{j,i}^{PIC} - z_{j,i}^{PIC,des} \\ z_{j,i}^{PIC,max} = (\beta_{m,k} + \beta_f) \times (a_{j,i}^{max} \times q_{j,i} + b_{j,i}^{max}) \\ z_{j,i}^{PIC,min} = (\beta_{m,k} + \beta_f) \times (a_{j,i}^{min} \times q_{j,i} + b_{j,i}^{min}) \\ z_{j,i}^{PIC,des} = (\beta_{m,k} + \beta_f) \times (a_{j,i}^{des} \times q_{j,i} + b_{j,i}^{des}) \end{cases}$$

$$(3)$$

with the objective function

$$\mathcal{J}_{n_P,k} := \sum_{i=0}^{n_P} \sum_{j=1}^{3} (q_{j,i} - r_{j,i}) Q_{j,i} (q_{j,i} - r_{j,i}) + $$
$$(m_i - m_{basal,i}) R_k (m_i - m_{basal,i}) + $$
$$e_{j,i}^{PIC} P_k e_{j,i}^{PIC}$$

where $z_{j,k} \in \mathbb{R}^{\bar{n}_x}$ and $q_{j,k} \in \mathbb{R}$ denote the predicted states and output, respectively, for the prediction/control horizon n_P, $m_k \in \mathbb{R}$ denotes the constrained input variable, taking values in a nonempty convex set $\mathcal{M}$ with $\mathcal{M} := \{m_k \in \mathbb{R} : m_{min,k} \le m_k \le m_{max,k}\}$, $m_{j,k}^{min} \in \mathbb{R}$ and $m_{j,k}^{max} \in \mathbb{R}$ denote the lower and upper bounds on the manipulated input, respectively, r_k is the target set-point, and $m_{basal,k}$ is the patient-specific basal insulin rate. The index $\mathbb{N}_0^{n_P}$ represents all integers in a set as $\mathbb{N}_0^{n_P} := \{0, \dots, n_P\}$. The nonempty convex set $\mathcal{Z}$ with $\mathcal{Z} := \left\{z_{j,k} \in \mathbb{R}^{\bar{n}_x} : z_{j,k}^{min} \le z_k \le z_{j,k}^{max}\right\}$, $z_{j,k}^{min} \in \mathbb{R}^{\bar{n}_x}$ and $z_{j,k}^{max} \in \mathbb{R}^{\bar{n}_x}$ denote the lower and upper bounds on state variables, respectively, with one of the states as the estimated PIC ($z_{j,k}^{PIC}$) that is constrained by the PIC bounds ($z_k^{PIC,max}, z_{j,k}^{PIC,min}$, and $z_{j,k}^{PIC,des}$) where the $z_{j,k}^{PIC,des}$ is

Table 1. Meal scenario for 30-days closed-loop experiment using mGIPsim

Meal	Range for values	
	Time	Amount (g)
Breakfast	[06:00, 07:00]	[40, 60]
Lunch	[12:00, 13:00]	[40, 60]
Dinner	[18:00, 19:00]	[40, 60]

Table 2. Exercise scenario for 30-days closed-loop experiment using mGIPsim

Exercise	Range for values		
	Time	Duration (min)	Power
Bicycling	[10:00, 11:00]	[30, 60]	[50, 90]
Bicycling	[16:00, 17:00]	[30, 60]	[50, 90]

the desired PIC value. The $\bar{n}_x$ is the number of states in the integrated glycemic model described by Eq. 1. Furthermore, $\hat{x}_{j,k}$ provides an initialization of the state vector, $Q_{j,k} \ge 0$ is a positive semi-definite symmetric matrix used to penalize the deviations of the outputs from their nominal set-point, and $R_k > 0$ is a strictly positive definite symmetric matrix to penalize the manipulated input variables. At each iteration, the quadratic programming problem in Eq. 3 is solved, and $u_k := m_0$ is the optimal solution implemented to infuse insulin over the current sampling interval with the MPC computation repeated at next sampling time using new CGM data and energy expenditure, updated states, and newly calculated penalty weights of the objective function.

3. RESULTS

A multivariable glucose-insulin-physiological variable dynamics simulator (mGIPsim) for type 1 diabetes developed at Illinois Institute of Technology is used to assess the performance of AL-MPC (Rashid et al. (2019)). A 30 days scenario with different daily meal and exercise times and amounts as detailed in Tables 1 and 2 is considered to test the proposed approach comprehensively. Daily meal and exercise times and characteristics change randomly every day within the ranges provided in Tables 1 and 2. The controller set-point is set at 110 mg/dL except during exercise it becomes 160 mg/dL. In addition to the CGM values, mGIPsim generates physiological variable signals that would be reported by noninvasive wearable devices. Aerobic exercises with stationary bicycle are considered for testing the mAP. The meal and physical activity information are not entered manually to the mAP system as the mAP controller is designed to regulate the GC in the presence of significant unknown disturbances such as unannounced meals and exercises. The energy expenditure values expressed as MET variations are computed by the simulator and used as input variable summarizing the physiological signals in response to physical activities in the mAP system. The quantitative evaluation of the closed-loop operation based on the proposed algorithms is presented in Table 3. The simulation results indicate that the mAP integrated with adaptation and learning algorithms is robust and reliable in learning and accommodating the patients' daily habits and activities. The average percentage of time spent in the target ranges of [70,140] mg/dL and [70,180] mg/dL are 50.4 % and 75.4

Table 3. Closed-loop simulation results for AL-MPC whole days

Subject	Percent of time in range					Statistics			
	< 70	[70, 140]	[70, 180]	> 180	> 250	Mean	SD	Min	Max
S1	0.0	45.4	74.0	26.0	0.0	153.8	35.8	85	247
S2	0.0	53.9	73.8	26.2	0.7	151.6	39.2	80	261
S3	0.0	52.6	77.0	23.0	0.0	146.6	35.7	103	236
S4	0.0	57.8	81.8	18.3	0.2	143.3	36.0	80	259
S5	0.0	61.6	82.0	18.0	0.6	140.3	37.5	74	262
S6	0.0	49.1	79.8	20.2	0.0	149.3	31.5	93	232
S7	0.0	59.2	82.6	17.4	0.0	141.9	33.0	92	237
S8	0.0	58.9	80.5	19.5	0.0	141.9	34.9	91	238
S9	0.0	41.6	67.4	32.6	3.0	162.0	42.1	89	268
S10	0.0	60.0	78.9	21.1	0.1	142.8	37.2	73	254
S11	0.0	49.2	75.6	24.4	1.0	151.1	41.3	74	266
S12	0.0	54.4	76.8	23.2	0.1	148.3	37.8	83	254
S13	0.0	40.3	70.8	29.2	0.1	157.8	37.1	98	252
S14	0.0	55.2	76.9	23.1	0.3	146.9	40.0	78	260
S15	0.0	46.3	77.5	22.5	0.0	151.1	32.7	96	243
S16	0.0	57.3	83.0	17.0	0.0	143.2	30.6	88	230
S17	0.0	53.4	75.8	24.2	0.0	146.4	39.2	88	250
S18	0.0	31.4	58.8	41.2	4.4	171.0	44.1	103	275
S19	0.0	47.8	79.4	20.6	0.0	149.7	32.7	91	242
S20	0.0	33.0	58.5	41.5	3.6	170.7	43.7	105	279
Average	0.0	50.4	75.4	24.5	0.7	150.5	37.1	88	252

Table 4. Total number of predicted hypo preventions by rescue carbohydrates for the whole simulation period (30 days) and the average total daily insulin (U) with AL-MPC (results for A-MPC without learning in parentheses)

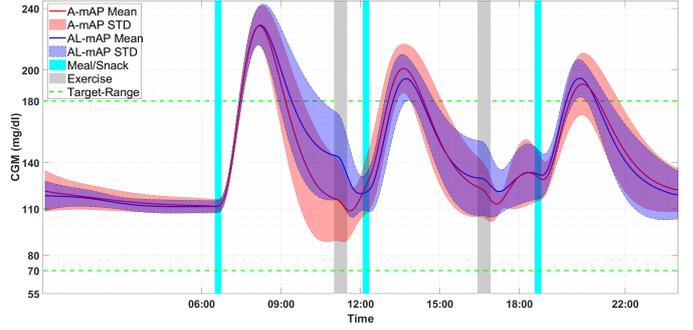| Subject	Number of predicted hypo	Total daily insulin (U)
S1	**11**(54)	**36.9**(39.6)
S2	**37**(105)	**35.7**(39.2)
S3	**6**(90)	**30.7**(33.9)
S4	**42**(95)	**31.8**(35.2)
S5	**80**(122)	**27.9**(29.8)
S6	**17**(63)	**38.2**(40.8)
S7	**27**(70)	**40.4**(42.7)
S8	**26**(89)	**29.6**(32.1)
S9	**10**(49)	**59.7**(63.3)
S10	**35**(75)	**27.9**(29.2)
S11	**38**(85)	**30.0**(32.1)
S12	**41**(78)	**25.5**(27.2)
S13	**4**(18)	**47.5**(47.6)
S14	**70**(119)	**28.5**(31.1)
S15	**7**(35)	**43.4**(44.9)
S16	**24**(100)	**41.9**(45.0)
S17	**61**(123)	**26.1**(28.0)
S18	**0**(12)	**49.2**(50.3)
S19	**27**(66)	**43.9**(46.5)
S20	**0**(7)	**42.8**(44.2)
Average	**28**(73)	**36.9**(39.1)

Fig. 4. Closed-loop results for all subjects on day 30
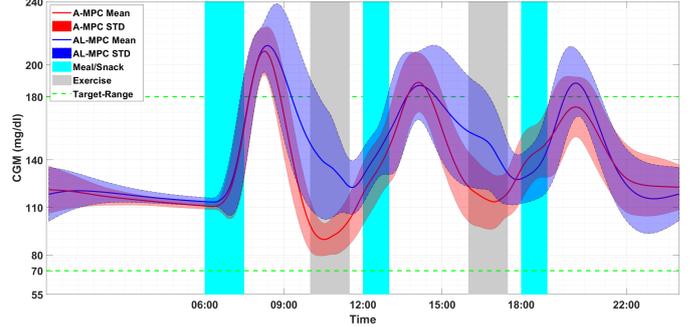

Fig. 5. Closed-loop results for one selected subject during whole simulation

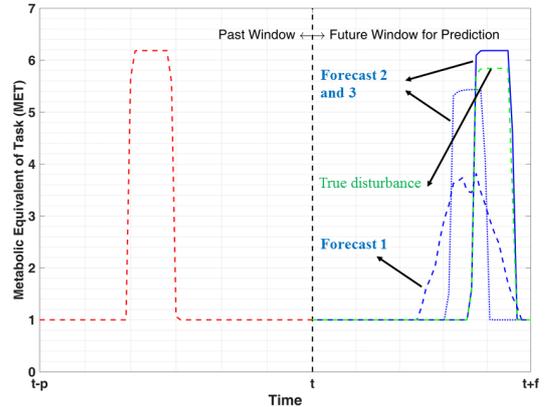Fig. 6. A sample of disturbance forecasts (MET) where t is the current time, p is the past window and f is the future window

% for all subjects. There is no hypoglycemia event as the GC is never below 70 mg/dL. The predicted hypoglycemic episodes warn the user to consume rescue carbohydrates about 20 minutes before the potential hypoglycemic episode. The average minimum and maximum observed GC values across all experiments during whole simulation are 88 and 252 mg/dL, respectively. Overall, the results illustrate that the proposed mAP with AL-MPC is able to regulate GC effectively in presence of significant unknown disturbances caused by the diverse times and amounts of meals and exercisetimes and intensities while mitigating severe hypo- and hyperglycemic excursions. The closed-loop results for all subjects for the last day of simulations shown in Fig. 4 shows that AL-mAP can proactively keep the CGM values in a higher range compared to the A-mAP (an adaptive mAP without the learning feature) during exercise periods. This is done by using a safe (higher) controller set-point in advance, which is determined based on MET forecasts that indicate the presence of exercise. For one selected subject, the closed-loop simulation results for all 30 days (Fig. 5) shows that integrating the learning feature with the mAP increases significantly the safety and reliability of the insulin delivery system specially during exercise periods. The glycemic control is improved over time as the learning technique modifies the controller parameters based on more comprehensive historical data (e.g. S9, S17, and S19). Overall, the AL-mAP system can also regulate the GC with a reduced need for hypoglycemia treatments (Table 4, average reduction from 73 to 28 hypoglycemic episodes that necessitate rescue carbohydrates are predicted). This

indicates that the calculated insulin doses are safer. A sample of disturbance forecasts for MET value is shown in Fig. 6. The forecasts of MET values can describe the real MET values accurately, which can be used for adjusting the key MPC parameters in advance for periods when exercise is predicted.

4. CONCLUSION

An adaptive MPC with learning ability is developed for controlling nonlinear processes with time-varying characteristics. The glucose-insulin dynamics in human body is used as the test system for illustrating the performance of the adaptive-learning MPC (AL-MPC). The AL-MPC framework integrates disturbance forecasting, uncertainty quantifications, learning, and recursive subspace identification. Machine learning captures trends in historical data to improve MPC performance. The results illustrate that blood glucose control can be improved further by using learning without causing undesirable effects or excessive interventions.

REFERENCES

Cheung, J.Y. and Stephanopoulos, G. (1990). Representation of process trendspart i. a formal representation framework. *Comput Chem Eng*, 14(4-5), 495–510.

Forbes, M.G., Patwardhan, R.S., Hamadah, H., and Gopaluni, R.B. (2015). Model predictive control in industry: Challenges and opportunities. *IFAC-PapersOnLine*, 48(8), 531 – 538. 9th IFAC Symposium on Advanced Control of Chemical Processes ADCHEM 2015.

Ganesh, H., Edgar, T., and Baldea, M. (2016). Model predictive control of the exit part temperature for an austenitization furnace. *Processes*, 4(4), 53.

Garcia, C.E., Prett, D.M., and Morari, M. (1989). Model predictive control: theory and practice–a survey. *Automatica*, 25(3), 335–348.

Garcia-Tirado, J., Corbett, J.P., Boiroux, D., Jørgensen, J.B., and Breton, M.D. (2019). Closed-loop control with unannounced exercise for adults with type 1 diabetes using the ensemble model predictive control. *J Process Control*, 80, 202–210.

Hajizadeh, I., Hobbs, N., Samadi, S., Sevil, M., Rashid, M., Brandt, R., Askari, M.R., Maloney, Z., and Cinar, A. (2019a). Controlling the AP controller: Controller performance assessment and modification. *J Diabetes Sci Technol*, 13(6), 1091–1104.

Hajizadeh, I., Rashid, M., and Cinar, A. (2018a). Integrating compartment models with recursive system identification. In *2018 Annual American Control Conference (ACC)*, 3583–3588. IEEE.

Hajizadeh, I., Rashid, M., and Cinar, A. (2019b). Plasma-insulin-cognizant adaptive model predictive control for artificial pancreas systems. *J Process Control*, 77, 97–113.

Hajizadeh, I., Rashid, M., Samadi, S., Sevil, M., Hobbs, N., Brandt, R., and Cinar, A. (2019c). Adaptive personalized multivariable artificial pancreas using plasma insulin estimates. *J Process Control*, 80, 26–40.

Hajizadeh, I., Rashid, M., Turksoy, K., Samadi, S., Feng, J., Sevil, M., Hobbs, N., Lazaro, C., Maloney, Z., Littlejohn, E., et al. (2018b). Incorporating Unannounced Meals and Exercise in Adaptive Learning of Personalized Models for Multivariable Artificial Pancreas Systems. *J Diabetes Sci Technol*, 12(5), 953–966.

Hajizadeh, I., Samadi, S., Sevil, M., Rashid, M., and Cinar, A. (2019d). Performance Assessment and Modification of an Adaptive Model Predictive Control for Automated Insulin Delivery by a Multivariable Artificial Pancreas. *Ind Eng Chem Res*, 58(26), 11506–11520.

Hartigan, J.A. and Wong, M.A. (1979). Algorithm as 136: A k-means clustering algorithm. *J R Stat Soc Ser C Appl Stat*, 28(1), 100–108.

Houtzager, I., van Wingerden, J., and Verhaegen, M. (2012). Recursive predictor-based subspace identification with application to the real-time closed-loop tracking of flutter. *IEEE Trans Control Syst Technol*, 20(4), 934–949.

Kanungo, T., Mount, D.M., Netanyahu, N.S., Piatko, C.D., Silverman, R., and Wu, A.Y. (2002). An efficient k-means clustering algorithm: Analysis and implementation. *IEEE Trans Pattern Anal Mach Intel*, (7), 881–892.

Kumar, R., Wenzel, M.J., Ellis, M.J., ElBsat, M.N., Drees, K.H., and Zavala, V.M. (2018). A stochastic model predictive control framework for stationary battery systems. *IEEE Trans Power Syst*, 33(4), 4397–4406.

Kumar, R., Jalving, J., Wenzel, M.J., Ellis, M.J., ElBsat, M.N., Drees, K.H., and Zavala, V.M. (2019a). Benchmarking stochastic and deterministic mpc: A case study in stationary battery systems. *AIChE Journal*, 65(7), e16551.

Kumar, R., Wenzel, M.J., Ellis, M.J., ElBsat, M.N., Drees, K.H., and Zavala, V.M. (2019b). Hierarchical mpc schemes for periodic systems using stochastic programming. *Automatica*, 107, 306 – 316.

Mayne, D.Q. (2014). Model predictive control: Recent developments and future promise. *Automatica*, 50(12), 2967–2986.

Mesbah, A., Paulson, J.A., Lakerveld, R., and Braatz, R.D. (2017). Model predictive control of an integrated continuous pharmaceutical manufacturing pilot plant. *Org Process Res Dev*, 21(6), 844–854.

Moharir, M., Pourkargar, D.B., Almansoori, A., and Daoutidis, P. (2018). Distributed model predictive control of an amine gas sweetening plant. *Ind Eng Chem Res*, 57(39), 13103–13115.

Perea-Lopez, E., Ydstie, B.E., and Grossmann, I.E. (2003). A model predictive control strategy for supply chain optimization. *Comput Chem Eng*, 27(8-9), 1201–1218.

Rashid, M., Samadi, S., Sevil, M., Hajizadeh, I., Kolodziej, P., Hobbs, N., Maloney, Z., Brandt, R., Feng, J., Park, M., Quinn, L., and Cinar, A. (2019). Simulation software for assessment of nonlinear and adaptive multivariable control algorithms: Glucose-insulin dynamics in Type 1 diabetes. *Comput Chem Eng*, 130, 106565.

Rawlings, J.B. and Mayne, D.Q. (2009). *Model predictive control: Theory and design*. Nob Hill Pub.

Wagstaff, K., Cardie, C., Rogers, S., Schrödl, S., et al. (2001). Constrained k-means clustering with background knowledge. In *Icml*, volume 1, 577–584.

Zavala, V.M. and Biegler, L.T. (2009). The advanced-step NMPC controller: Optimality, stability and robustness. *Automatica*, 45(1), 86–93.